Energy 264 (2023) 126142

Contents lists available at ScienceDirect

Energy

journal homepage: www.elsevier.com/locate/energy

Exergy assessment and sustainability of a simple off-shore oscillating water column device

A. Molina-Salas [a,*], C. Quirós [b], P. Gigant [c], F. Huertas-Fernández [a], M. Clavero [a], A. Moñino [a]

[a] Andalusian Institute for Earth System Research, Universidad de Granada, Av. del Mediterráneo s/n, 18006, Granada, Spain
[b] IDOM Consulting Engineering and Architecture, Project Engineer, Sevilla, Spain
[c] INSA Lyon, Department of Energy and Environmental Engineering, 20 Avenue Albert Einstein, 69621 Villeurbanne Cedex, France

ARTICLE INFO

Keywords:
Wave energy
Oscillating water column
Thermodynamics
Renewability
Exergy
Renewability index

ABSTRACT

This paper present a research on the performance efficiency and sustainability of an Oscillating Water Column (OWC) simple off-shore device, accounting for the influence of governing thermodynamic variables (moisture, temperature, pressure) in the compression/expansion polytropic process. The work proposes a simple off-shore OWC experimental set up as the basis of the study. The analysis takes into consideration both gas subsystems inside and outside the OWC, to achieve a better understanding of the conservative nature of entropy system variable, the net exchange balance, the effects on efficiency and exergy destruction, and the interpretation of the OWC as a thermodynamic engine. Results show that, within the context of the set up, moderate wave climate conditions contribute to a better efficiency of the device in terms of output power, providing with a low impact on exergy destruction and high sustainability in terms of renewability index.

1. Introduction

The ocean dynamics represents a source of clean energy with continuous availability for primary conversion. Focusing on the wave energy resource, the estimates suggest an accessible power up to $\sim 10^7$ MW for off-shore harvesting along the coasts worldwide, Falnes [1] and Cruz [2]. Focusing in the case of Europe, the estimates offer an available wave power of $3.2 \cdot 10^5$ MW, O'Hagan et al. [3]. Accounting for the fact that the global renewable primary conversion in Europe represents ~34%, World Energy Council [4], wave resource appears to be a key factor in the energy budget. Still on the european frame, even if the estimates for 2020 are of ~170 MW of installed power from wave and tidal resources, that value is still far from the expected capacity accounted for circa 2009 by the National Renewable Action plans, Magagna and Uihlein [5]. In the context of a world climate change scenario, it is necessary to conduct a deep research in order to bridge technical, economical and environmental gaps, and to make the ocean resource an alternative to fossil primary conversion, as well as an attractive and profitable field for stakeholders and investors, SI Ocean [6,7,8].

One of the most interesting technological alternatives for wave energy converters (WEC) is the oscillating water column (OWC), to which a considerable amount of research has been devoted during the past decades, Cruz [2] and Falcão [9]. The OWC concept lies on a hollow chamber, partially submerged and opened to the sea at the bottom to allow transmission of wave momentum and energy to the interior. The wave action compresses and expands the air system inside the chamber and drives the power take-off system (PTO), usually consisting of a Wells turbine, Gato and Falcão [10] and Raghunathan [11]. The Wells turbine provides linearity between pressure drop and flow discharge, and reversibility in rotation induced by flow direction. The process of compression/expansion of the gas system inside the chamber transform the wave energy into electricity through pneumatic action on the PTO turbine.

The fundamentals of the OWC performance have been theoretically developed within the context of Linear Theory, providing with a complete analytical description from the scope of the radiation–diffraction problem, Evans [12], Sarmento and Falcão [13] and Evans and Porter [14]. Studies have been focused to take into account the OWC performance in terms of its placement with respect to coastal structures, Martins-Rivas and Mei [15], Martins-Rivas and Mei [16] and Lovas et al. [17], and to integrate them in vertical breakwaters [18]. Research has been conducted on the PTO control and performance efficiency and management, Gato and Falcão [19], Justino and Falcão [20], Falcão and Justino [21], Carballo et al. [22] and Falcão et al. [23], on the interaction between PTO damping and tidal-wave climate, López et al. [24,25], or on the interaction between OWC and seabed morphology and the consequences for the long-term performance, Rezanejad et al. [26,27] and Medina-López et al. [28,29].

* Corresponding author.
E-mail address: amsalas@ugr.es (A. Molina-Salas).

https://doi.org/10.1016/j.energy.2022.126142
Received 12 April 2022; Received in revised form 22 October 2022; Accepted 18 November 2022
Available online 22 November 2022

List of Symbols

A_a	Total cross section area occupied by the blades – [m^2]
A_b	Turbine blades area – [m^2]
A_t	Cross section area of the turbine – [m^2]
B	Second virial coefficient – [–]
$\tilde{B}$	non-dimensional radiation coefficient of the radiation problem – [–]
$\tilde{C}$	non-dimensional added mass coefficient of the radiation problem – [–]
c	Chord length of the blade – [m]
C_p	Specific heat under constant pressure – [J/mol K]
C_p^*	Specific heat under constant pressure for the ideal gas – [J/mol K]
$\tilde{C}_p$	Non-dimensional specific heat under constant pressure – [–]
C_v	Specific heat under constant volume – [J/mol K]
C_v^*	Specific heat under constant volume for ideal gas – [J/mol K]
$\tilde{C}_v$	Non-dimensional specific heat under constant volume – [–]
D_{OWC}	OWC device diameter – [m]
D_t	Diameter of the turbine – [m]
e_v	Vapour pressure – [Pa]
e	Unitary exergy – [J/mol]
$e_{1\to0}$	Unitary exergy from state 1 to 0 – [J/mol]
$e_{1\to2}$	Unitary exergy from state 1 to 2 – [J/mol]
$\tilde{e}_{1\to2}$	Non-dimensional exergy from state 1 to 2 – [–]
e_{da}	Needed exergy to the deactivation of possible generated waste in the process – [J/mol]
e_{dp}	Exergy rate related to waste disposal of the process – [J/mol]
e_{dt}	Destroyed exergy in the complete process – [J/mol]
e_{em}	Exergy of the wastes that are emitted to the atmosphere – [J/mol]
e_{nr}	Exergy of non-renewable fuel – [J/mol]
e_{out}	Exergy of the products – [J/mol]
H	Enthalpy – [J]
H_s	Wave heigh – [m]
h_w	mean level water depth – [m]
h	Specific enthalpy – [J/kg]
h^*	Specific enthalpy for the ideal gas – [J/kg]
$\tilde{h}$	Non-dimensional specific enthalpy – [–]
h_0	Specific enthalpy of the environment – [J[kg]]
h_1, h_2	Specific enthalpy of the states 1 and 2 – [J/kg]
k	Wave number – [rad/m]
kh	Relative depth – [–]
kL	Capture length – [–]
L	Work done on the system – [J]
$L_{0,unit}^{irrev}$	Unitary irreversible work done on the system – [J]
$L_{0,unit}^{rev}$	Unitary reversible work done on the system – [J]
N	Turbine rotation velocity – [r.p.m.]
p	Static pressure – [Pa]
p_{tot}	Total pressure – [Pa]
p_c	Critical pressure – [Pa]
Q	Volumetric air flow rate – [m^3/s]
Q	Heat exchanged – [J]
q_0	Specific heat exchanged between the auxiliar system and the environment – [J/mol]
q_1, q_2	Specific heat exchanged between the auxiliar system and the inlet and outlet systems – [J/mol]
q_R	Specific heat rejected by the auxiliar system – [J/mol]
R_0	Universal gas constant – [8.31 J/K mol]
R_a	Air gas constant – [286.7 J/K mol]
R_{ext}	External turbine radius – [m]
RH	Relative humidity – [–]
R_{int}	Internal turbine radius – [m]
R_{med}	Turbine average radius – [m]
R_{OWC}	OWC device radius – [m]
R_v	Water vapour constant – [461 J/K kg]
r	Mixing ratio – [–]
s^*	Unitary entropy for an ideal gas – [J/K mol]
$\tilde{s}$	Non-dimensional unitary entropy – [–]
s_0	Unitary entropy of the environment – [J/K mol]
S_1, S_2	Entropy of the states 1 and 2 – [J/K]
s_1, s_2	Unitary entropy of the states 1 and 2 – [J/mol K]
T_z	Wave period – [s]
T	Temperature – [K]
$T_0, T1, T2$	Temperature of the environment and states 1 and 2 – [K]
T_c	Critical temperature – [K]
U	Internal energy – [J]
U	Air flow velocity – [m/s]
U_{in}	Axial component of the flow through the chamber – [m/s]
U_{tip}	Blade circumferential velocity at blade tip – [m/s]
U_y	Vertical component of flow velocity – [m/s]
v_m	Molar volume – [m^3/mol]
W^*	Non-dimensional pneumatic power output – [–]

Greek

Δs	Unitary entropy increment – [J/mol K]
$\Delta\tilde{s}$	Non-dimensional entropy increment – [–]
Δs^{irr}	Unitary entropy due to irreversibility – [J/mol K]
ΔU	Internal energy increment – [J]
$\tilde{\Gamma}$	Non-dimensional diffraction coefficient of the diffraction problem – [–]
η	Efficiency – [–]
η_e	Exergy efficiency – [–]
η_{pneu}	Pneumatic efficiency – [–]
eta^{rev}	Efficiency of the reversible engine – [–]
λ	Renewability index – [–]
Π_0	Non-dimensional group – [–]
ρ	Density – [kg/m^3]
σ	Turbine solidity – [–]
Φ^*	Non-dimensional discharge through the turbine – [–]

Numerical and experimental knowledge has led to an examination of OWC features under simulation scenarios otherwise difficult to observe without full scale prototypes, such as the fundamentals of aerodynamic and hydrodynamic coupling, Teixeira et al. [30], the OWC efficiency under non linear considerations, Luo et al. [31], or the improvement of OWC simulation models by means of the implementation of the Actuator Disk Model theory for turbine simulation, Moñino et al. [32], to cite some studies. Without going in further details, at the time of writing

this, research efforts are dedicated to advance in the improvement of the PTO turbine performance, Halder and Samad [33], Lopes et al. [34], Cui et al. [35] and Liu et al. [36].

Power plants relying on OWC technology can be found worldwide, either as full-scale prototypes or production oriented: PICO (Portugal), Mutriku (Spain), LIMPET (Scotland), Tofftestallen (Norway), Port Kembla (Australia), Sakata, Kujukuri, Sanze and Niigata (Japan), Vizhinjam (India), Shanwei and Dawanshan (China), to cite some examples. Those experiences indicate that OWC technology can be a feasible reality for wave energy extraction, although important challenges has to be faced. Valuable information can be extracted form those projects concerning performance and efficiency, The Carbon Trust [37]. Nonetheless, there remain economical, technical and social facts to be circumvented when bridging the wide gap between design and final deployment and connection to the grid, ranging from creating an attractive market for investors, to minimize installation costs and to satisfy end-users instead of creating a Not In my Backyard (NIMBY) effect [6–8,38–40].

One of the big challenges in the development of an easy-to-deploy cost-competitive OWC technology, is to balance the overall efficiency values. While predicted efficiency for OWC plants can be estimated around 40% or higher, observed values reach only 10%, The Carbon Trust [37], with obvious implications not only in the design and deployment process, but also on the levelised cost of energy (LCOE) comprising the ratio between capital and operation expenditures (CAPEX and OPEX respectively). As a first outcome, a ratio of 5 million Euro per 1 installed MW can be currently assigned, de Andres et al. [41], or even higher for off-shore harvesting, National Ocean Economic Program [42]. However that point should not mean a withdrawal in the use of WECs in general and OWCs in particular, but rather a revision on the design and management criteria. While devices are designed for high energy wave climate, say, $\gtrsim 50$ kW/m, the reality is that the current WEC projects and prototype deployments work under mild climate conditions, Magagna and Uihlein [5]. Indeed, authors have come up with results showing that the efficiency of OWC devices is higher for performances under moderate climate conditions, Jalón et al. [43]. That is the case, for example, of Mediterranean areas, with annual mean significant wave heights under ~ 1.5 m, [44]. Hence, climate and operative conditions alongside with the fact that more than 60% of WEC projects are off-shore oriented, Magagna and Uihlein [5], must be considered as a starting point of a design and development policy in which the objective is a cost-effective and simpler device design with shorter service life, easier to maintain, repair and replace and, more important, with better efficiency for mild energy resources.

One important point to set the limits of the OWC cycle and the performance and efficiency of the PTO turbine is the Thermodynamics of the air chamber. The characteristics of the compression/expansion polytropic process and the nature of the gas inside the chamber, actually a mixture of dry air and water vapour with specific partial pressure and density, plays a role in the pneumatic efficiency (air cycle to turbine rotation conversion) of the WEC and hence in the global efficiency calculated as the product of the hydraulic (impinging wave to air cycle conversion) and pneumatic efficiencies. Indeed, the influence of the nature of the fluid on the turbine efficiency is well known in the field of gas turbines in thermal power plants (Rahman et al. [45], Kim et al. [46], Yang and Su [47] and Singh and Kumar [48]).

The common yet adequate approach to the compression/expansion process – and its subsequent coupling with the radiation–diffraction theory – assumes an adiabatic polytropic process of an ideal gas, Falcão and Justino [21], Zhang et al. [49] and Sheng et al. [50]. However, a feasible contribution to explain the low OWC efficiency values as indicated above can be found by the implementation of a real gas model. If the standard thermodynamic formulation is enhanced by the implementation of the state equation corrected by a virial Kammerlingh–Onnes expansion, Gayé [51], Prausnitz et al. [52], Wisniak [53] and Tsonopoulos and Heidman [54], the reduction in the efficiency can be better explained. Preliminary experiments on stationary air–water vapour flow and numerical solutions of the radiation–diffraction problem with real gas implementation point in that direction, Medina-López et al. [55,56,57].

Furthermore, climate and operative conditions as discussed above, as well as technical factors, hast to be kept into account for the development of policies in which sustainability, reduction of carbon footprint and cost-effective design stand out as the main objectives. In the previous sense, the OWC represents a sustainable primary conversion technology with low exergy destruction, high renewability and reduced carbon footprint, that can be implemented as part of sustainable low-emission production-clean plants such as hydrogen electrolysis plants, Huertas-Fernández et al. [58]. According to the foregoing discussion, the focus is placed on simpler device design with shorter service life, easier to maintain, repair and replace, with better efficiency for mild energy resources and low rates of exergy destruction, Rosen [59], Sciubba [60] and de Oliveira [61].

The objective of this paper is to conduct a preliminary assessment on the sustainability of the wave energy extraction through OWC technology, based on the exergy analysis as a reliable way to evaluate the effective energetic yield and the straightforward impact on the renewability. The paper is organized as follows. In the first place, a theoretical development of the exergy concept will be made, as well as a thermodynamic description of the process. Afterwards, the experimental setup of the tests to estimate the exergy variation will be described. And finally, results will be exposed and discussed, with the conclusions and the possible future researches.

2. Theoretical background

2.1. Exergy and renewability index

The exergy can be defined as a thermodynamic state function representing the maximum work capacity rendered by a system in equilibrium with the environment, Sciubba [60] and de Oliveira [61]. The exergy analysis of an energy production system – a thermodynamic engine with its auxiliar system if preferred – can provide with helpful information in terms of sustainability, regarding the maximum useful work that can be attained from the transformation of a primary resource, by ultimately seizing the rejected heat which is consequence of the Second Principle of Thermodynamics, as discussed in Appendix. Indeed, the exergy budget for the OWC converter can be developed following the classical formulation of the exergetic balance for a general system and accounting for the specific features involved in compression and expansion processes.

A thermodynamic engine is considered according to the scheme in Fig. 1, following the concepts and fundamentals in de Oliveira [61]. The auxiliar system AS – whose concept has been defined in Appendix – represents an engine operating between unitary heat sources q_1 and q_2 under temperatures T_1 and T_2, enthalpies h_1 and h_2, and entropies s_1 and s_2 (all of them expressed in J/mol), rendering an unitary work L^{irr}_{unit} otherwise irreversible in general terms, and rejecting an unitary heat q_R. The maximum work rendered by the AS engine can be maximized using for the purpose a reversible engine, for example a Carnot engine, operated by an auxiliar system ASR, between the rejected heat q_R and the environment heat q_0, rendering an amount of reversible work $L^{rev}_{0\,unit}$. The concept of Carnot engine results very helpful given the fact that according to the Carnot Theorem, the efficiency of any thermodynamic engine operating between heat sources is lower than the efficiency of a Carnot engine operating between the same sources, Gayé [51].

Both the systems AS and ASR can be considered as subsystems of a global engine GE operating between several heat sources and transforming it into work. Ultimately, the engine represented in Fig. 1 describes a general system at large driven by energy/chemical/mass flow sources/outputs – sources q_1 and q_2 –, in which there are production units – auxiliar systems – operating under generally irreversible conditions, alongside with other units that can be in equilibrium with

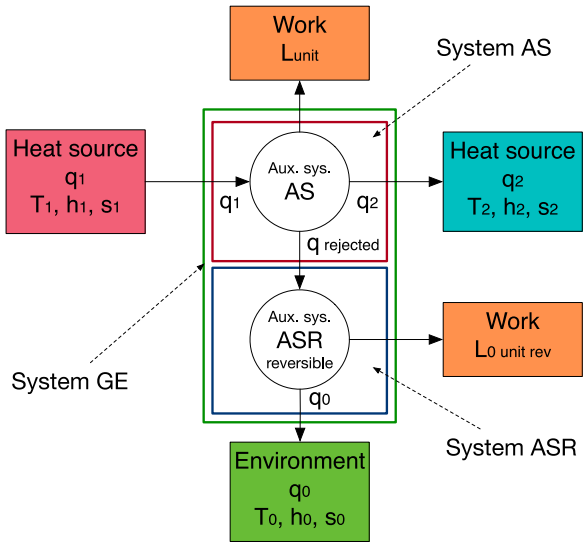

Fig. 1. Thermodynamic engine GE comprising an engine AS operating between unitary heat sources q_{in} an q_{out}, and using the rejected heat q to operate a Carnot engine ASR connected to the environment q_0.

the environment under an essentially reversible condition, generating an amount of energy/work with additional losses. As it will be discussed later, that would be the starting point to draw the similitudes with an OWC device, for example.

Now the First Principle of Thermodynamics is applied to the global engine GE and to the Carnot engine ASR solely, as a first step to quantify the efficiency of the engine in terms of the available conditions, respectively leading to:

$$q_0 = h_2 - h_1 + L^{irr}_{unit} + L^{rev}_{0\,unit} \tag{1}$$

and:

$$q_R - q_0 = L^{rev}_{0\,unit} \tag{2}$$

following the convention of received heat as positive and rejected heat as negative.

The Second Principle applied to the Carnot engine ASR reveals that the heat balance over a complete cycle of the ASR equals 0 due to reversibility. Hence:

$$\oint \frac{dq_{total}}{T} = 0 = \int_1^2 \frac{dq}{T} - \frac{q_0}{T_0} \Rightarrow \int_{in}^{out} \frac{dq}{T} = \frac{q_0}{T_0} \tag{3}$$

Additionally, the Second Principle considering the irreversible AS operating between states (q_1, h_1, s_1, T_1) and (q_2, h_2, s_2, T_2) leads to:

$$s_2 - s_1 \geqslant \int_{in}^{out} \frac{dq}{T} \tag{4}$$

which implies that for the relation to become an equality, an extra amount of generated entropy Δs^{irr} due to irreversibility has to be added to the balance of heat:

$$s_2 - s_1 = \int_1^2 \frac{dq}{T} + \Delta s^{irr} \tag{5}$$

Equating (3) and (5):

$$q_0 = T_0(s_2 - s_1) + T_0 \Delta s^{irr} \tag{6}$$

and combining with (1) and clearing out:

$$h_1 - h_2 - T_0(s_1 - s_2) = L^{irr}_{unit} + L^{rev}_{0\,unit} + T_0 \Delta s^{irr} \tag{7}$$

The Eq. (7) can be expressed in a more convenient form recalling the efficiency of the reversible engine ASR, and accounting for (2) and (3):

$$\eta^{rev} = \frac{L^{rev}_{0\,unit}}{q} = 1 - \frac{q_0}{q_R} = 1 - \frac{T_0}{q_R} \int_1^2 \frac{dq}{T} \tag{8}$$

hence:

$$h_1 - h_2 - T_0(s_1 - s_2) = L^{irr}_{unit} + q\eta^{rev} + T_0 \Delta s^{irr} \tag{9}$$

The expression (9) represents [right side] the amount of work – both reversible and irreversible – that can be obtained from the system operating between sources [left side] $(q_1,\ h_1)$ and $(q_2,\ h_2)$ and exchanging heat q_0 with the environment, plus an extra generation of entropy from irreversible processes involved, Δs^{irr}. The expression (9) can be regarded as a measure of the availability of useful work that can be obtained from a source – heat, chemical, mass flow – at a given state, accounting for the losses due to irreversibility involved at certain levels within the production/transformation process. Therefore, the specific exergy at the input of the general system GE as represented in Fig. 1 can be defined as the balance of energy and entropy from input to output:

$$e_{1\to 2} = h_1 - h_2 - T_0(s_1 - s_2) \tag{10}$$

According to the concept of exergy, the greater the irreversibility features in a given production process – such as expansions with uncontrolled heat exchange, dissipation, combustion, etc. – the lower the capacity to generate reversible work for a given value of input exergy $e_{1\to 2}$, hence the lower the renewability as it shall be discussed later.

In addition, if the AS also operates as a reversible engine, then according to (3) and (4) the source of entropy due to irreversibility vanishes, i.e. $\Delta s^{irr} = 0$, and from (3) and (5):

$$s_2 - s_1 = \frac{q_0}{T_0} \tag{11}$$

which in turn is equivalent to assume that the general engine GE is in equilibrium with the environment. In that case the potentially available work is maximum according to (9), and it can be obtained from the general expression (10):

$$e_{1\to 0} \equiv h_1 - h_0 - T_0(s_1 - s_0) = L^{rev}_{unit} + q\eta^{rev} = L_{unit\,max} \tag{12}$$

or if preferred, the unitary exergy $e_{1\to 0}$ at the input represents in this case the maximum capacity that can be obtained from the environment to yield useful work:

$$e_{1\to 0} = h_1 - h_0 - T_0(s_1 - s_0) \tag{13}$$

A more adequate interpretation of the concept of exergy following expressions in (10), (12) and (13), can be utterly attained from the standpoint of irreversibility and exergy destruction, hence loss of capacity to get reversible energy from input resources. Indeed, the change in exergy between input and output states is in direct proportion to the variation of entropy:

$$e_{in\to out} \sim -T_0(s_{in} - s_{out}) \sim T_0(s_{out} - s_{in}) \sim T_0 \Delta s \tag{14}$$

An increment in entropy $\Delta s > 0$ therefore implies a destruction of exergy between input and output states, i.e. $e_{in\to out} > 0$.

Therefore, the exergy efficiency can be defined as the balance between exergy outputs and inputs, Sciubba [60] and de Oliveira [61]:

$$\eta_e = \frac{e_{outputs}}{e_{inputs}} \tag{15}$$

where output and input states must be understood as a set of processes associated with a given engine or converter system, in which the energy production at a given stage, serves as input to the next stage where that energy is used and so on. In addition, the exergy efficiency can be expressed in a more convenient form, in which the availability of reversible energy, i.e. the counterpart of exergy destruction, can be calculated. Thinking in terms of a thermodynamic engine as depicted in

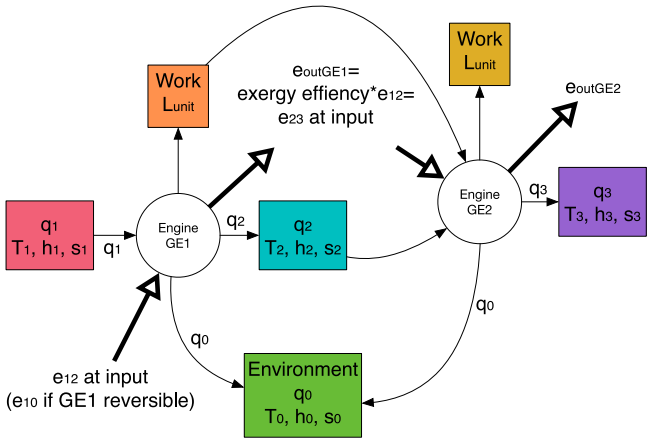

Fig. 2. Thermodynamic engines GE1 and GE2 and exergy flow through production line.

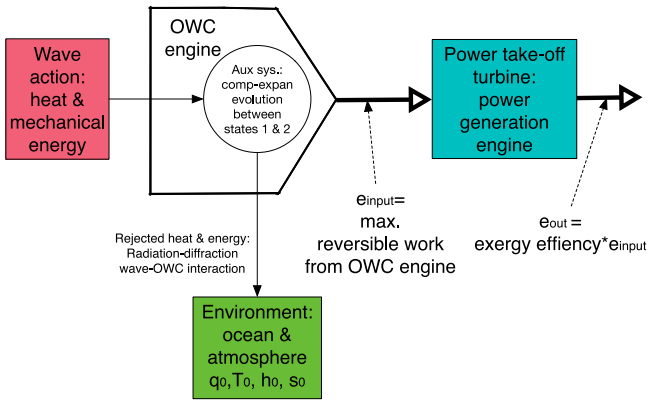

Fig. 3. Approach to the OWC device as a thermodynamic engine concept.

the schemes in Fig. A.18, the efficiency can be expressed in the general form, Gayé [51]:

$$\eta = 1 - \frac{\text{losses}}{\text{input energy}} \tag{16}$$

which takes the general quantitative form of a balance between a perfect efficiency and the expected losses in the form of exchanged heat according to the Second Principle of Thermodynamics. Therefore, it is feasible to express the exergy efficiency in a similar form:

$$\eta_e = 1 - \frac{\text{exergy destruction at products}}{\text{exergy destruction at sources}} \tag{17}$$

In this case the expression (15) represents the available exergy for reversible work production, with respect to the ideal situation in which all the input energy sources be transformed into useful work without heat losses, say, a 100% renewable and thermally isolated process in which according to expression (14) there would be no destruction of exergy and $\eta_e = 1$, as will be discussed later in this research.

It is clear that following the scheme of the GE engine in Fig. 1, the output flows – heat, work – from a given engine GE1 can be used as the input to another engine GE2, Fig. 2, as part of a higher-order production line. In any case, the exergy balance involves both the input exergy e_{in} and the exergy outputs through sequenced states of production.

In the general case represented in Fig. 2, accordingly to the expression (17) the exergy efficiency would be calculated as:

$$\eta_e = 1 - \frac{e_{outGE1} + \cdots}{e_{1\to 2}} \tag{18}$$

Furthermore, to relate exergy with the impact that a process may have on the environment and to account for exergy destruction, the renewability index (hereinafter RI) λ is proposed by de Oliveira [61] and Arredondo et al. [62], see Eq. (19). In fact, the concept of sustainability can be defined in different ways. One possibility is using the RI. This way allows to define the sustainability concept through the state variables of the system, which gives an objective yet accurate definition of this concept. Furthermore, this definition of the term *sustainability* allows to compare the indexes associated to other energy transformation and further production processes. RI takes into account the balance between exergy at outputs and exergy destruction from non renewable sources as well as the wastes generated by the process and its treatment, as function of exergy efficiency. Processes with $0 \leq \lambda < 1$ are environmentally unfavourable, processes with $\lambda \geq 1$ are environmentally favourable and when λ tends to ∞ it means that the process is reversible with renewable inputs and no wastes generated.

$$\lambda = \frac{\sum e_{out}}{e_{nr} + e_{dt} + e_{da} + e_{dp} + \sum e_{em}} \tag{19}$$

where: e_{out}: exergy of products, e_{nr}: exergy of non renewable fuel, e_{dt}: destroyed exergy in the complete process, e_{da}: exergy due to the deactivation of possible generated waste in the process, e_{dp}: exergy rate or flow rate related to waste disposal of the process, e_{em}: the exergy of wastes that are emitted to the atmosphere. According to expression (19) and following de Oliveira [61], the RI can be written in the case of the wave energy conversion in a more representative form as (20).

$$\lambda = \frac{\eta_e}{1 - \eta_e} \tag{20}$$

2.2. Exergy balance for the OWC system

In the case of the OWC device considered as a thermodynamic engine, the auxiliar system AS is represented by the gas inside the chamber, and the wave action drives the OWC compression/expansion cycle. The mixture of dry air and water vapour undergoes a compression/expansion process forced by the wave action. The AS takes the energy from the ocean environment, evolves through a compression/expansion cycle and returns to the initial state, rejecting an amount of energy to the environment. Whether that energy is returned entirely to the environment or is delivered between the environment and the OWC structure, it depends on the isolation restraints. In any case, even assuming the energy is preserved and hence the enthalpy, the entropy varies through the compression and expansion cycles, as a consequence of temperature, moisture and density variations, heat exchange and eventually irreversible stages during the process, leading to exergy destruction. According to the foregoing discussion, a feasible thermodynamic concept of the OWC engine can be represented following the scheme in Fig. 3.

The concept of exergy at the inlet of the system obviously depends on, and is consequence of, its definition as a thermodynamic state function with respect to a reference state, i.e. a given stage in a production line such as the generalization in Fig. 2. It is clear that if the OWC is considered as the power supply to some ultimate transformation/production engine in a production line, its associated exergy may represent different sources:

- In view of the OWC as an engine for electrical power supply, then the exergy at the input of the high-level production line would be $e_{1\to 2}$, following the scheme in Fig. 2 and Eq. (10).
- If the OWC is considered as a primary converter engine in which the gas system yields an amount of reversible work to be delivered to the power take-off turbine and generator, then the OWC itself – the useful work it produces – represents the exergy at the input of the production line, to be later delivered for electric power generation and further use. The OWC would perform in that case as a primary thermodynamic engine in equilibrium with the ocean environment, and its corresponding exergy would be essentially $e_{1\to 0}$ according to Fig. 3 and Eq. (13).

Fig. 4. Wave flume built inside the wave basin for the purpose.

In both cases, a cyclical process will occur in which there will be a change in entropy, and, therefore, an exergy destruction. Considering the OWC as a primary converter engine (engine GE1 in Fig. 2), the exergy $e_{1\to 0}$ represents the maximum reversible work given that the system is in equilibrium with the environment and interacts only with this environment. So, the amount of work that the PTO turbine will receive (considering the PTO system as the engine GE2 in Fig. 2) from the OWC system will always be the maximum available. In the case of primary conversion, expression (17) would implement $\eta_{pneu} \cdot e_{1\to 0}$ as exergy variation of the product – i.e. exergy destruction –, where η_{pneu} is the pneumatic efficiency of the OWC device. This η_{pneu} would be obtained from the capture length according to the radiation–diffraction theory, Sarmento and Falcão [13] and Martins-Rivas and Mei [15].

2.3. Thermodynamic state functions

Following the foregoing discussion, the auxiliar system AS in the OWC thermodynamic engine consists of a mixture of dry air and water vapour. The Thermodynamic formalism can be applied to the air–water vapour mixture assumed as a real gas, to derive system function relationships between thermodynamic states reached through the AS process, ultimately required for the assessment of exergy balance and renewability index. The formulation rationale of the real gas state functions and coupling between real gas performance and radiation–diffraction theory can be checked in Medina-López et al. [56,57] and Moñino et al. [63]. For the sake of simplicity, only the thermodynamics functions describing the real gas will be presented in Appendix.

3. Experimental set up

The experimental study is conducted in the facilities at the Hydraulics Laboratory in the School of Civil Engineering, University of Granada (Spain). The set up consists of a wave flume 10 m long × 1.5 m wide with a flat horizontal bottom, built for the purpose inside the wave generation basin and isolated from the surrounding waterbody by a solid wall. With that configuration, two of the sixteen paddles featured in the wave basin are dedicated to wave generation inside the flume — see Fig. 4. The depth of the still water is set to $h_w = 0.4$ m for all tests. A dissipative beach is built at the end of the flume in order to minimize wave reflection interaction with incident waves generated from the paddles. All in all, the focus is placed on the direct interaction between surface level oscillations inside the chamber and thermodynamic processes during compression/expansion cycles. The wave propagation is recorded through seven wave gauges located on positions windward (2.6 m, 1.8 m and 1.5 m from the OWC), leeward (1 m, 1.8 m and 2.1 m from the OWC) and inside the OWC chamber — see Fig. 5 for details.

The off-shore OWC converter model consists of a hollow vertical cylindrical structure 0.93 m high with an internal diameter $D_{owc} = 0.2$ m. Two 0.05 m height gaps are made at the base, spanning along the perimeter of the cylinder to allow wave transmission between windward, leeward and inner OWC chamber regions. The air chamber inside the OWC is 0.33 m high, ending at the top in a cone-shaped transition to the 0.08 m diameter and 0.1 m height cylindrical shaft housing the turbine – see Fig. 6 for details –. The turbine used is a linear No–Wells type turbine, whose characteristics are: diameter $D_t = 0.025$ m, cross section area $A_t = 3.5906 \cdot 10^{-4}$ m^2 (centre to blade tip), blades area $A_b = 2.4271 \cdot 10^{-4}$ m^2, solidity $\sigma = 0.7315$. The turbine performance – details on calibration can be found in Moñino et al. [63] – can be represented by a linear relationship between pressure drop Δp and both rotation velocity N [r.p.m.] or the air flow Q [m^3/s]. This relation is shown in expression (21a) and (21b):

$$\Delta P = 1.1125 \cdot 10^6 \cdot Q - 292.875 \tag{21a}$$

$$\Delta P = 98.4 \cdot 10^{-3} \cdot N - 126.1 \tag{21b}$$

Thermodynamic and flow-related variables (temperature T, humidity RH, static pressure p, total pressure p_{tot}) are measured in and outside the OWC chamber. Some details on the configuration of pressure taps and temperature and humidity probes set up are represented in Fig. 7. A total of ten taps are used for static and total pressure recording in the OWC device. Five taps are placed outside the chamber and another five are embedded inside the turbine shaft, following the scheme depicted in Fig. 6. The pressure taps are connected to a *DTC Initium* pressure transducer system configured at a sampling rate of 250 Hz, with an accuracy of ±5%. The measurement of the temperature and moisture have been made with two *Vaisala INTERCAP HMP60* probes measurement range: 0%–100% in relative humidity, and −40 – +60 °C in temperature, with an accuracy of ±5% in relative humidity and ±7% in temperature. Both the wave gauges and temperature and moisture probes are connected to a data acquisition system configured at 50 Hz. In all cases the sampling frequency ensures appropriate observation of high-frequency phenomena as derived from the Nyquist Theorem. In addition, one pressure tap is connected to a piezometer attached to wave gauge WG1 – see Fig. 5 –, to check time matching between water surface elevation, temperature, moisture and pressure series.

4. Results and discussion

For the present study the key factor is how the wave action is captured by the device for a range of wave-number values, and how the associated energy is transferred into the thermodynamic compression/expansion air system process, regardless the rate of reflection superimposed to the impinging waves. Indeed, regular waves are run for the tests summarized in Table 1, with no active wave absorption enabled since the flume is equipped with a dissipative beach.

The Table 2 shows the geometric characteristics of the turbine and the air properties, respectively.

4.1. Isolation between OWC and out gas systems

One important factor in the compression/expansion process under wave induced flow in the OWC, is the extent to which the PTO turbine works as a kind of thermodynamic restraint for the gas system inside

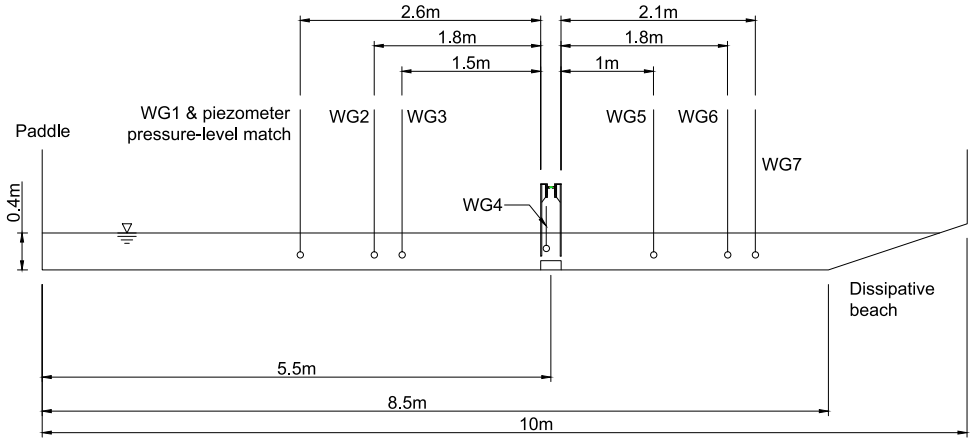

Fig. 5. General set up and wave gauges location.

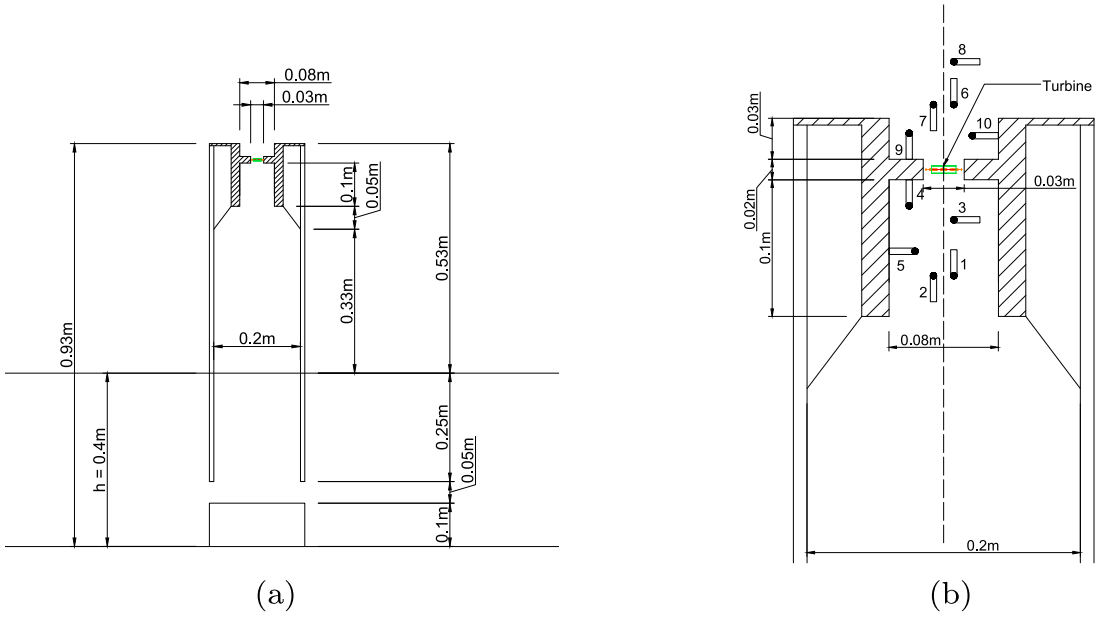

Fig. 6. OWC set up. (a): geometrical configuration. (b): cross section and pressure taps configuration.

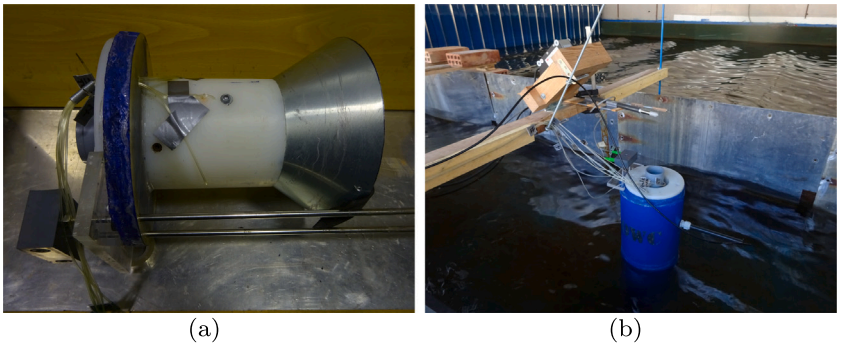

Fig. 7. OWC configuration. (a): gauges and taps set up: inner cone-shaped transition and cylindrical shaft with embedded taps and wave gauge WG4 (inside OWC chamber), and taps connection and temperature/humidity probes. (b): general view and cylindrical shaft housing the turbine.

the chamber, the nature of it yet to be determined (heat insulation, mass exchange insulation, etc.). However, some information can be advanced from the analysis of the experimental OWC performance. For the sake of simplicity, the following discussion focuses on the tests cases 4 ($H_s = 0.05$ m, $T_z = 1.58$ s), 7 ($H_s = 0.1$ m, $T_z = 2.21$ s) and 9 ($H_s = 0.15$ m, $T_z = 2.21$ s) according to Table 1.

The analysis of thermodynamic variables of pressure p, moisture RH, temperature T and density ρ_{gas} time series on locations inside the OWC chamber and outside the turbine, reveals that there exists in fact an isolation between inside and outside regions in terms of temperature and moisture, see Fig. 8 for the test case 7 ($H_s = 0.1$ m, $T_z = 2.21$ s) (the rest of test cases exhibit similar response).

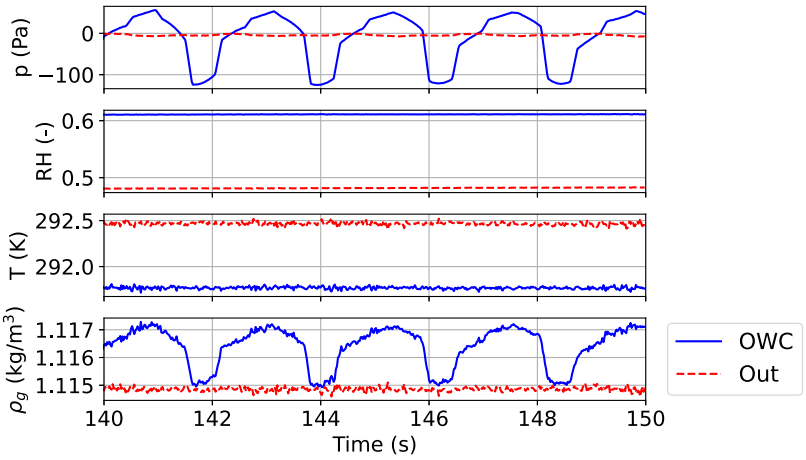

Fig. 8. Thermodynamic variables inside the OWC chamber and outside the turbine. Data for case 7 ($H_s = 0.1$ m, $T_z = 2.21$ s).

Table 1
Test runs for regular waves (water depth $h = 0.4$ m).

Test	Wave height H_s [m]	Wave period T_z [s]	Wave number kh [–]
1	0.1	2	0.68
2	0.05	0.95	1.87
3	0.05	1.26	1.21
4	0.05	1.58	0.90
5	0.1	1.58	0.90
6	0.1	1.90	0.72
7	0.1	2.21	0.61
8	0.15	1.90	0.72
9	0.15	2.21	0.61
10	0.15	2.53	0.52

Table 2
Left: Turbine geometry specifications. Right: Dry air and water vapour properties.

Property	Value	Value	Units
R_{int}	0.0025 m	Air properties	
R_{ext}	0.0125 m	R_a	286.7 J/kg K
R_{med}	0.0075 m	$C_{p,a}$	1010 J/kg K
D_t	0.025 m	ρ_a	1.25 kg/m^3
A_t	$3.5906 \cdot 10^{-4}$ m^2	MW_a	0.0288 kg/mole
c	0.0049 m	$T_{c,a}$	132 K
A_a	$2.427 \cdot 10^{-4}$ m^2	$p_{c,a}$	$37.71 \cdot 10^5$ Pa
σ	0.7315	Water vapour properties	
Number of blades	7	R_v	461 J/kg K
Turbine type	Linear No–Wells	$C_{p,v}$	1093 J/kg K
Profile of the blades	Flat	MW_v	0.0182 kg/mole
		$T_{c,v}$	647 K
		$p_{c,v}$	$220.89 \cdot 10^5$ Pa

The temperature and moisture series indicate that the values inside the OWC and outside the turbine remain essentially constant. In the case of test 7 ($H_s = 0.1$ m, $T_z = 2.21$ s), the values fall around $T_{OWC} \simeq 291.8$ K and $RH_{OWC} \simeq 61\%$, and $T_{out} \simeq 292.5$ K and $RH_{out} \simeq 49\%$ respectively. Alike response is observed in the rest of test cases described in Table 1. The gas inside the OWC is cooler and more humid that the gas outside, and so remains through all the wave series. However, it seems from the data that there is no mixing between inside and outside gas subsystems, as far as the respective RH values remains constant, i.e. there is no addition or loss of water vapour to the gas system mixture. There should be any effective mixing between OWC and out gas subsystems, that would be accompanied by a variation in the temperature and humidity of the mixture, which is not the case. Therefore it can be concluded that, at least in terms of local thermodynamics, the turbine performance implies an effective temperature and humidity isolation between OWC and out subsystems.

It is relevant to note that the change in gas density ρ_{gas} inside the OWC can be explained from the properties of the dry air–water vapour mixture, rather than from a mixing process with a gas of different water vapour concentration. Indeed, according to Medina-López et al. [55], the density of the dry air–water vapour mixture, ρ_g, depends on the mixing ratio r, and this in turn depends on the vapour pressure, e_v, and the thermodynamic pressure of the mixture p_g. The vapour pressure depends on the temperature only, which remains constant (see Fig. 8), and therefore, the vapour pressure remains constant. Thus, the only variable that modifies the mixing ratio is p_g, which implies that the only variable that affects the density of the dry air–water vapour mixture ρ_g is the pressure of the dry air–water vapour mixture.

Moreover, it seems clear from the pattern represented in Fig. 8 that the gas subsystem outside the chamber performs as a manostat, in the sense that the OWC pressure p_g sets the conditions to drive the flow through the turbine during compression and expansion cycles, while the pressure remains essentially constant outside. That condition can also be checked from the time series of static pressure p (thermodynamic pressure) vs. vertical component U_y of flow velocity, both in OWC and out regions, see Fig. 9. According to the results, the time variations in p_{OWC} force the variation in U_{yOWC} and U_{yout} during compression (positive values) and expansion (negative values), both of them essentially inside the same range of magnitude. However, the area outside the chamber remains essentially under manometric $p_{out} \simeq 0$, i.e. under atmospheric pressure conditions.

The preservation of p_{out} essentially constant during both compression and expansion implies that the approach to the thermodynamic process has to be done in a different way as it has been for the OWC under stationary flow, Moñino et al. [63]. Nonetheless, the conclusions reached in that research regarding real gas performance and influence on efficiency continue to be valid. Indeed, the governing factors are now the oscillatory flow and the manostat condition set by p_{out} and *isolated* from the gas subsystem inside the OWC through the turbine itself. Hence the complete compression/expansion cycle can be interpreted as a thermodynamic process consisting of a sequence of equilibrium states, represented as a *closed* curve in the pressure–volume thermodynamic space, hereinafter $p-V$ space. The prediction of *intermediate equilibrium states* in that cycle has to be conducted on the analysis of system variables through state equations inside the OWC chamber, rather than between states inside and outside as it would be done in the case of pure stationary flow – in which a given control volume evolves between inside the OWC and outside the turbine at each given instant, see Moñino et al. [63] –.

To put it bluntly, it seems that the turbine performs like a kind of insulating wall, allowing the OWC gas system to work as a simple

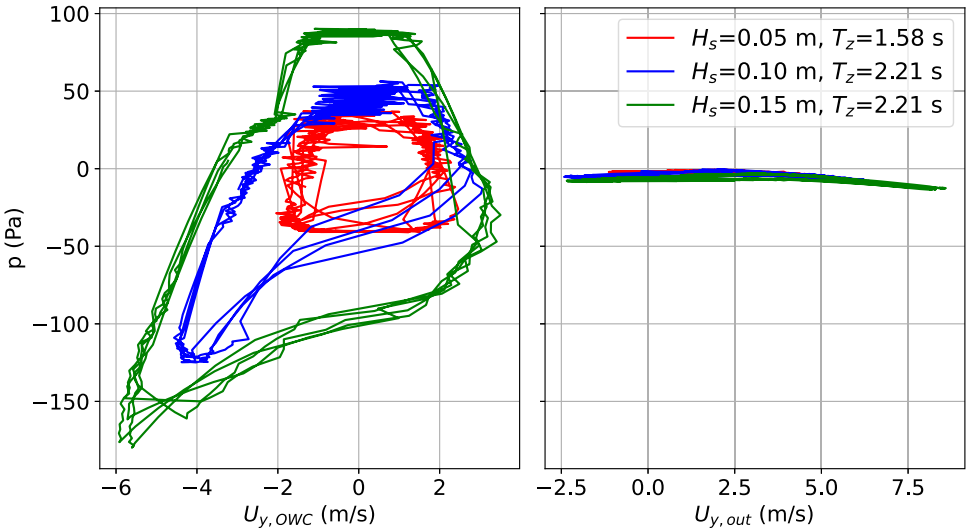

Fig. 9. Manometric pressure vs. vertical component of flow velocity in OWC (left) and out (right).

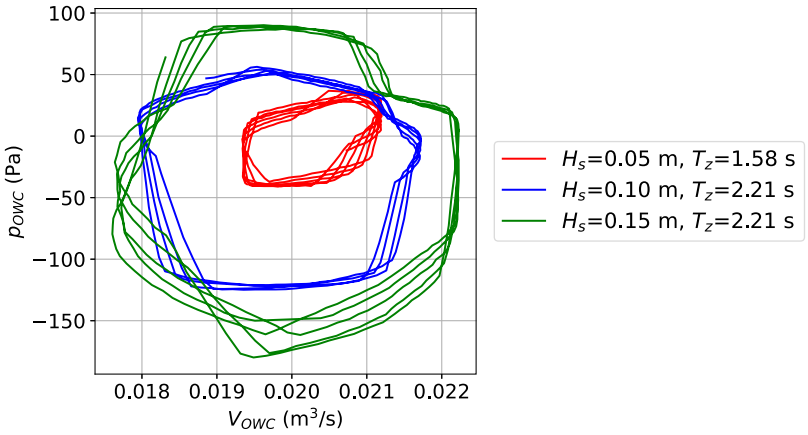

Fig. 10. Gas volume inside the OWC vs. manometric pressure.

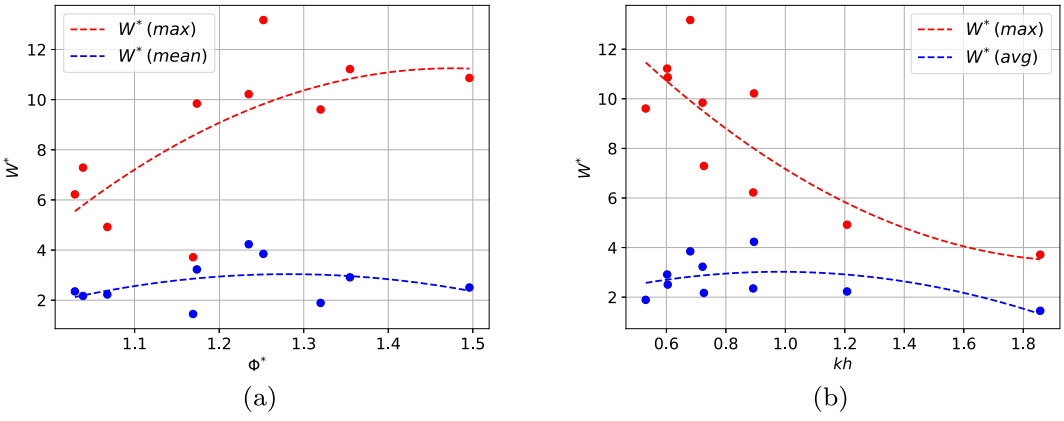

Fig. 11. (a): non-dimensional pneumatic power vs. non-dimensional flow. (b): non-dimensional pneumatic power vs. relative depth.

closed system according with previous findings, Molina-Salas et al. [64]. Evidences can be found on the following. On one hand, the different values of relative humidity and temperature between OWC and outer regions, which remain constant. On the other hand, the pressure outside the chamber remains constant, performing as a manostat with $p_{out} \simeq 0$. The foregoing discussion can be pictured in a clearer way through the representation of states in the $p-V$ space, Fig. 10.

4.2. Power output

The non-dimensional values of pressure p^*_{owc} are represented versus the non-dimensional flow discharge ϕ^* in Fig. 11. The non-dimensional pressure can be defined as:

$$p^*_{owc} = \frac{p_{owc}}{\rho_{owc} U^2_{tip}} \left(\frac{1 - RH_{owc}}{RH_{out}} \right) \tag{22}$$

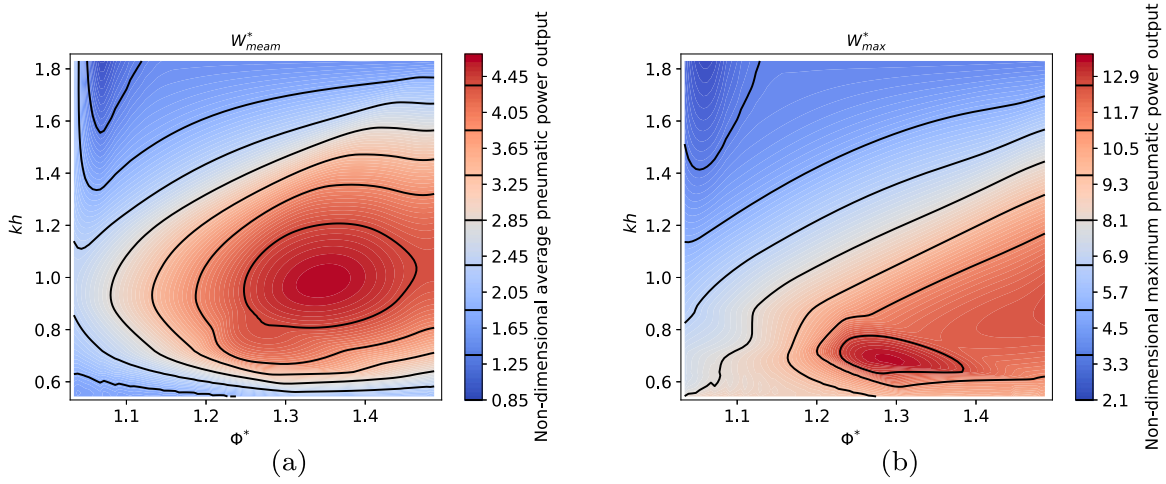

Fig. 12. Non-dimensional available pneumatic power as a function of relative depth and non-dimensional flow. (a): mean value. (b): maximum value.

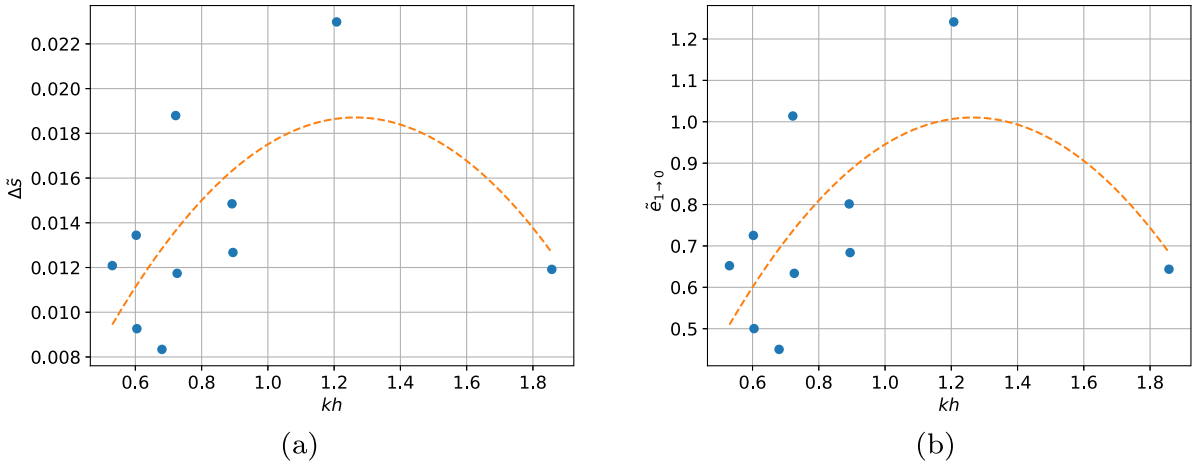

Fig. 13. (a): non-dimensional entropy vs. relative depth. (b): non-dimensional exergy vs. relative depth.

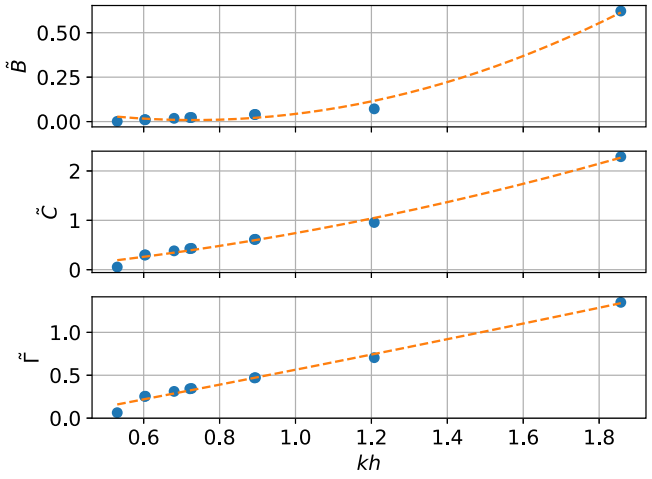

Fig. 14. Radiation–diffraction coefficients.

where p_{owc} is the manometric pressure inside the chamber, ρ_{owc} is the density of the air–water vapour mixture inside the chamber, U_{tip} is the tangential velocity at the tip of the turbine rotor, and RH_{owc} and RH_{out} are the relative humidities in and outside the chamber. The non-dimensional flow discharge is defined as:

$$\phi^* = \frac{U_{in}}{U_{tip}} \tag{23}$$

where U_{in} is the axial component of the flow through the chamber.

Following the expressions (22) and (23), the available pneumatic power can be calculated as:

$$W^*_{owc} = p^*_{owc}\phi^* \tag{24}$$

Fig. 11 shows the maximum and mean non-dimensional pneumatic power output. It can be observed how, according to Eq. (24), the maximum non-dimensional pneumatic power output increases with the increment of the non-dimensional flow. This result is consistent with previous results obtained by the authors, Moñino et al. [63]. However, the mean non-dimensional pneumatic power output remains approximately constant for the entire range of values of the non-dimensional flow, ranging between $W^*_{mean} \sim 2-3$. A similar behaviour is observed when the non-dimensional pneumatic power output is represented against the relative depth. It shows how the maximum non-dimensional pneumatic power output decreases with the increasing value of the relative depth, while the mean non-dimensional pneumatic power output remains practically constant. The complete relative dependence between W^*, kh and ϕ^* is represented in the contours of Fig. 12 .

It can be highlighted that the average pneumatic power output availability (to be later converted into electrical power) exhibit a

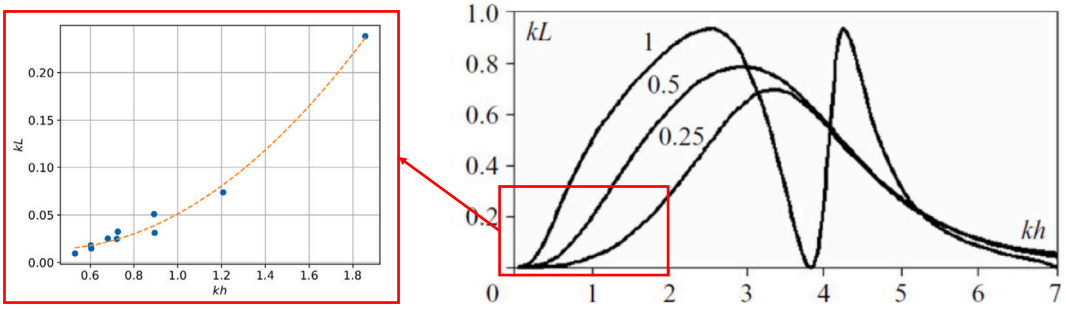

Fig. 15. Capture length. vs relative depth. Left: values obtained for the present research. Right: result obtained by Martins-Rivas and Mei [15, figure 6]. In the right panel the numbers 1, 0.5 and 0.25 indicates the relation between the radius of the OWC chamber and the depth of the still water. The experimental tests correspond with the value of 0.25.

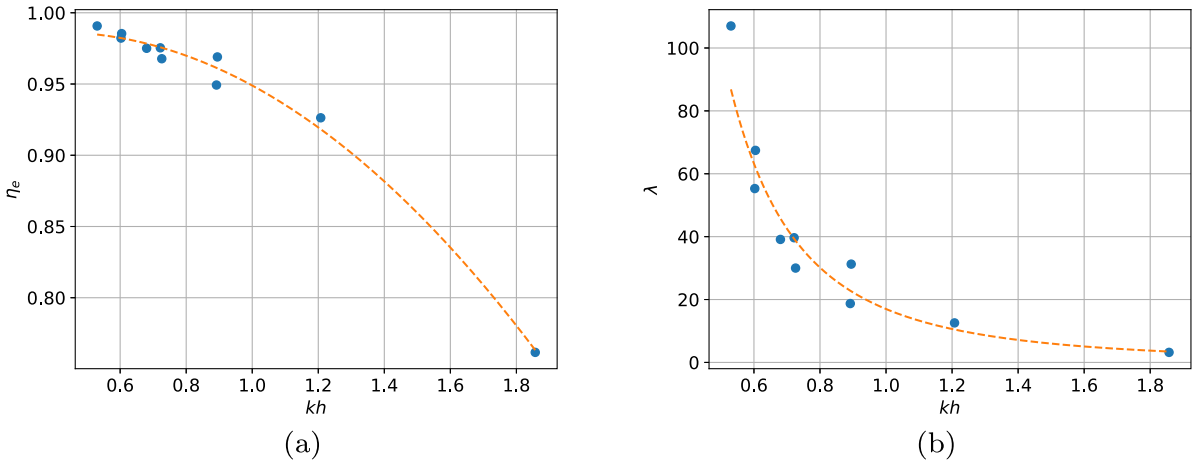

Fig. 16. (a) Exergy efficiency vs. relative depth. (b) Renewability index vs. relative depth.

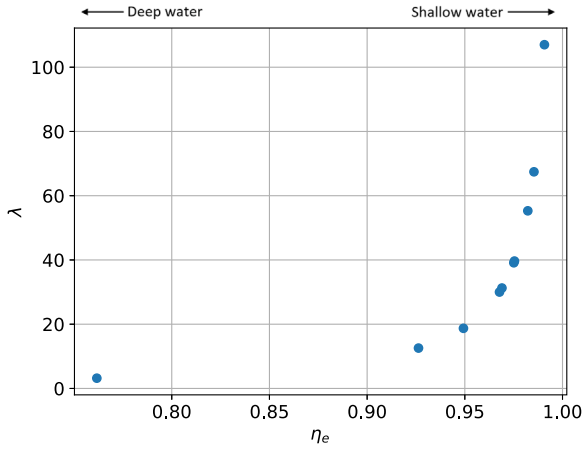

Fig. 17. Renewability index vs. exergy efficiency.

smooth variation on the range of both kh and ϕ^*. This behaviour suggests that the device performance with an essentially uniform efficiency for a wide range of kh, i.e., wave climate conditions. This fact supports the results obtained in previous researches – Jalón et al. [43] – which indicates that the efficiency of OWC devices is higher for performances under moderate climate conditions, since the average pneumatic power output is constant for a wide range of wave conditions.

4.3. Exergy efficiency and renewability index

To obtain the renewability index, the first step is to analyse the entropy and exergy variation in each wave cycle, which are shown in Fig. 13. It can be observed that the entropy variation depends on the value of the relative depth. The maximum entropy variation, i.e., the maximum irreversibility in the process of compression/expansion, is attained for a value of $kh \sim 1.2$. The variation of exergy $e_{1\to0}$ is proportional to the variation of entropy, so the exergy destruction has the same behaviour than the entropy variation, reaching its maximum value at $kh \sim 1.2$.

As indicated in Section 2.2, the exergy efficiency can be obtained from expression (18) as:

$$\eta_e = 1 - \frac{\eta_{pneu} \cdot e_{1\to0}}{e_{1\to0}} \equiv 1 - \eta_{pneu} = 1 - kL \tag{25}$$

where kL is the capture length according to expression (26) – Martins-Rivas and Mei [15] –, where coefficients $\tilde{B}$, $\tilde{C}$ and $\tilde{\Gamma}$ can be obtained from Fig. 14, following previous researches by the authors, Medina-López et al. [57]. The relation between the capture length and the relative depth is shown in Fig. 15. It can be observed how the higher the relative depth, the higher the capture length. This figure is consistent with the results obtained by Martins-Rivas and Mei [15, figure 6]. According to these two figures, the values of the capture length – i.e., the pneumatic efficiency – for the observed range are low not because the device efficiency itself, but because of the value of the relative depth considered. According to Martins-Rivas and Mei [15, figure 6], for a relation of $R_{owc}/h = 0.25$ between OWC radius and the water depth corresponding to this research, the pneumatic efficiency value would reach a maximum around $kh \sim 3.5$. Therefore, it can be expected that the pneumatic efficiency of the device increases up to ~0.7 when the value of kh increases to ~3.5.

$$kL = \frac{gka}{\omega C_g} \frac{\chi|\tilde{\Gamma}|^2}{\left(\chi + \tilde{B}\right)^2 + \left(\tilde{C} + \beta\right)^2} \tag{26}$$

Nevertheless, even though the value of kL increases with the increment of kh, the exergy efficiency decreases, as shown in Fig. 16.

Indeed, the higher the kh, the more energy the device is capable to capture, but with a lower exergy efficiency. The exergy efficiency reveals that the conversion from wave energy to available energy for turbine motion, in the sense of the percentage of energy from waves that can be converted into useful work, would be less reversible, thus increasing the destruction of exergy.

Following expression (20), the renewability index λ can be calculated as represented in Fig. 16. As the exergy efficiency decreases, the renewability index decreases as expected, since the destruction of exergy – i.e. the irreversibility – increases. Nevertheless, even for the lower exergy efficiency, or the higher irreversibility if preferred, $\lambda \to\sim 3$, which means that following de Oliveira [61], the device is environmentally favourable, given $\lambda > 1$ for any value of relative depth. That value is in accordance with estimations by the authors in previous researches, Huertas-Fernández et al. [58].

Fig. 17 shows the relation between the exergy efficiency and λ. As $\eta_e \to 1$, the value of λ tends to infinity. According to the definition of the exergy efficiency, the higher the value of η_e, the higher the reversibility in capturing of energy, so the higher the exergy of the products. All in all, η_e does not reveal the amount of energy the device can capture, rather than the amount of energy that can really be used. So, according to Fig. 15, although the device can capture a low amount of energy from the ocean when the relative depth decrease (as shown in Fig. 15), the transformation of this energy into available useful work is higher for shallow water than for deep water.

5. Conclusions and future research

In this research, the performance efficiency, reversibility and sustainability of an OWC device has been studied through the exergy analysis, in order to obtain the renewability index of the device for the primary conversion. The main conclusion of this research are:

- The turbine works as a restrain for the gas system inside the chamber since there is no mixing between the inside and outside OWC chamber gas subsystems in terms of temperature and relative humidity.
- The non-dimensional average pneumatic power output remains essentially constant for the considered range of relative depth.
- The higher the relative depth, the higher the captured energy by the device, but the lower the relative available useful work that can be obtained in a reversible way. Although the pneumatic efficiency increases with increasing relative depth, the exergy efficiency decreases, hence the irreversibility of the energy extraction process. All in all, the exergy destruction for any kh quantitatively represents the intrinsic capacity of the OWC device to capture the wave energy resource in a reversible way.
- The higher the exergy efficiency, the higher the renewability index. So when the exergy efficiency tends to the value of 1, the renewability index tends to infinity.
- The exergy efficiency and therefore the renewability index, are higher in shallow water than in deep water, which means that the reversibility in the wave energy primary conversion process from the environment is higher in the shallow water. In any case, the renewability index for a simple off-shore OWC device as proposed in this research, can be considered as environmentally favourable according to values of $\lambda \gg 1$. Considering a conventional power plant using coal as fuel, the λ values range from 0.18 to 0.43.[1]

Next steps spinning from this research are: (i) To verify the influence of the turbine characteristics. This will allow to set the reach of the results obtained in this research. (ii) To study a wider range of relative depth, in order to check the tendency shown for the different parameters analysed and compare with previous researches. (iii) To test different sizes of turbine with different geometries of the OWC chamber, in order to check the influence in the compression/expansion process. (iv) To study the scale effects in order to be able to extend the results to a full-scale prototype.

[1] According to de Oliveira [61].

CRediT authorship contribution statement

A. Molina-Salas: Research, Analysis, Writing and editing. **C. Quirós:** Background Research, Experimental setup. **P. Gigant:** Experimental setup. **F. Huertas-Fernández:** Research, Analysis, Writing and editing. **M. Clavero:** Project leading, Setup supervision, Manuscript revision. **A. Moñino:** Project leading, Concept, Setup supervision, Writing and editing.

Declaration of competing interest

The authors declare that they have no known competing financial interests or personal relationships that could have appeared to influence the work reported in this paper.

Data availability

The authors do not have permission to share data.

Acknowledgements

This work was funded by Andalusian Regional Government, Spain, projects P18-RT-3595 and B-RNM-346-UGR18. Research to be continued under grant TED2021-131717B-I00 funded by MCIN/AEI/10.13039/501100011033 and, as appropriate, by ERDF A way of making Europe, by he European Union and by the European Union NextGenerationEU/PRTR.

Appendix. Thermodynamic background

First and second principles of thermodynamics

The First Principle of Thermodynamics states that the amount of work L required for a thermal isolated system to evolve from an initial state to a final one does not depend on the process itself, but only on the initial and final states, Gayé [51]. In other words, the balance ΔU of internal energy between states is equal to the adiabatic work exerted on the system, say:

$$\Delta U = L^{adiab} \tag{A.1}$$

When the process is not adiabatic, the difference between ΔU and the work exerted on the system equals the heat Q exchanged with the ambient, so that:

$$\Delta U = Q + L = L^{adiab} \tag{A.2}$$

The Second Principle of Thermodynamics states that it is not possible the transformation of heat into work only, which implies that there is always an extra amount of exchanged heat (take/yield) which is required for a system to operate.

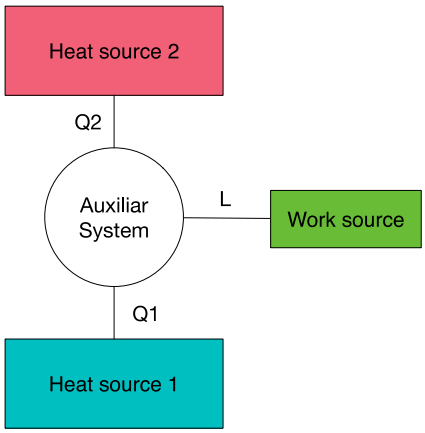

Fig. A.18. General scheme of a thermodynamic engine.

Thermodynamic machine

A thermodynamic engine can be defined, Gayé [51], as a device in which a so called *auxiliar system*, hereinafter AS, takes/yields an amount of heat (energy) from various heat sources, and yields/takes an amount of work (energy) from several work sources and yields/takes an amount of heat (energy) from several heat sources, Fig. A.18. The AS consists of a simple closed system following a cyclic process, so the initial and final states are the same (a concept which in turn implies reversibility), and exchanging energy from several sources as described above. The AS addresses the First and Second Principles of Thermodynamics as expected. The efficiency of the thermodynamic engine as described, is the balance between the desired output and the required input.

It is interesting to draw the similitude between the OWC–PTO system and a *thermodynamic engine* for the purpose of this research. The OWC concept as thermodynamic engine spins off as a natural consequence from the early findings by the authors, related with the thermodynamics of the gas system itself. The sequence of pressure–volume states – the polytropic process – through which the gas system evolves, determines the energy extraction and the efficiency in terms of the pressure work and heat budget, in turn related with the global efficiency of the OWC.

Entropy

The natural consequences of the Second Principle of Thermodynamics along with the concept of thermodynamic machine, are the Carnot Theorem, the definition of the thermodynamic temperature as a state function, the Clausius Theorem and the ultimate definition of entropy as a state function, Gayé [51].

The Carnot Theorem states that any thermodynamic machine operating between two heat sources cannot yield more efficiency that a Carnot machine – a machine whose auxiliar system as defined in Appendix undergoes a Carnot cycle – operating between the same heat sources.

The Clausius Theorem states that any system undergoing any cyclic process in which a certain amount of heat Q can be exchanged under temperature T follows the relationship:

$$\oint \frac{dQ}{T} \leqslant 0 \tag{A.3}$$

being equal to 0 if the process is reversible. The consequence of (A.3) is that a state function named *entropy* can be defined for any given process between states 1 and 2 in the form:

$$\int_1^2 \frac{dQ}{T} \leqslant S_2 - S_1 \tag{A.4}$$

which becomes an equality if the process is reversible. On the other hand, if the process is adiabatic there is no heat exchange, and it follows from (A.4):

$$S_2 - S_1 \geqslant 0 \tag{A.5}$$

Thermodynamic state functions

The specific heats under constant pressure and volume, C_p and C_v respectively, molar enthalpy h and molar – or unitary if preferred – entropy s, can be derived from the implementation of the real gas formalism and the virial expansion – please refer to Gayé [51] for further details on the rationale –. Therefore, using "*" for the ideal gas functions, it can be deduced the following expressions for the specific heat C_p:

$$C_p = C_p^* - Tp\frac{d^2B}{dT^2} \rightarrow [\text{J/mol K}] \tag{A.6}$$

specific heat C_v:

$$C_v = C_v^* - \frac{R_0}{v_m}\frac{d}{dT}\left(T^2\frac{dB}{dT}\right) \rightarrow [\text{J/mol K}] \tag{A.7}$$

molar enthalpy:

$$h = h^* + Bp - T\frac{dB}{dT}p \rightarrow [\text{J/mol}] \tag{A.8}$$

and molar entropy:

$$\Delta s = \Delta s^* - p\frac{dB}{dT} \rightarrow [\text{J/mol K}] \tag{A.9}$$

where B represents the second virial coefficient, according to Tsonopoulos and Heidman [54], Gayé [51], Moñino et al. [63], and it is a function of the temperature.

The molar enthalpy h^* of the ideal gas can be expressed as a function of the specific heat C_p^* and the flow velocity U:

$$h^* = C_p^* T + \frac{1}{2}U^2 \tag{A.10}$$

In the case of the molar entropy of the ideal gas s^*, the variation between states can be defined as:

$$\Delta s^* = C_p \ln\frac{T_2}{T_1} - R_0 \ln\frac{p_2}{p_1} \tag{A.11}$$

Therefore, considering the *Tsonopoulos innovation* (Tsonopoulos and Heidman [54]), the state functions of the real gas from (A.6) to (A.9) can be completely determined for any given thermodynamic state.

The state functions for specific heats, enthalpy and entropy can be conveniently expressed in non-dimensional form for further analysis. Indeed, application to the Pi Theorem to the thermodynamic problem results in the deduction of a common non-dimensional group:

$$\Pi_0 = \frac{TR_0}{pB} \tag{A.12}$$

to be used as repeated factor in the non-dimensional expressions of C_p, C_v, h and Δs:

$$\tilde{C}_p = \left|\frac{T}{pB}\right| C_p \tag{A.13}$$

$$\tilde{C}_v = \left|\frac{T}{pB}\right| C_v \tag{A.14}$$

$$\tilde{h} = \left|\frac{1}{pB}\right| h \tag{A.15}$$

$$\tilde{\Delta s} = \left|\frac{T^2R_0}{p^2Bv_m}\right| \Delta s \tag{A.16}$$

Finally, according to the definition of exergy in expression (14) (expressed in J/mol, according to the International System), the non-dimensional expression of exergy is:

$$\tilde{e}_{in\rightarrow out} = \left|\frac{TR_0}{p^2Bv_m}\right| e_{in\rightarrow out} \tag{A.17}$$

References

[1] Falnes J. A review of wave-energy extraction. Mar Struct 2007;20(4):185–201.
[2] Cruz J. Ocean wave energy. Current status and future perspectives. Springer–Verlag; 2008, p. 431.
[3] O'Hagan AM, Huertas C, O'Callaghan J, Greaves D. Wave energy in Europe: Views on experiences and progress to date. Int J Mar Energy 2016;14:180–97.
[4] World Energy Council. World energy resources 2016. World Energy Council; 2016, p. 1028, ISBN: 978-970-946121-58-8.
[5] Magagna D, Uihlein A. Ocean energy development in europe: Current status and future perspectives. Int J Mar Energy 2015;11:84–104.
[6] SI Ocean. Ocean energy: state of the art. Tech. Report, Brussels (Belgium): Strategic Initiative for Ocean Energy (SI Ocean); 2012, p. 78.
[7] SI Ocean. Ocean energy technology: gaps and barriers. Tech. Report, Brussels (Belgium): Strategic Initiative for Ocean Energy (SI Ocean); 2012, p. 64.
[8] SI Ocean. Ocean energy: cost of energy and cost reduction opportunities. Tech. report, Brussels (Belgium): Strategic Initiative for Ocean Energy (SI Ocean); 2013, p. 29.
[9] Falcão AFde O. Wave energy utilization: A review of the technologies. Renew Sustain Energy Rev 2010;14(3):899–918.
[10] Gato LMC, Falcão AFde O. On the theory of the wells turbine. Trans ASME 1984;106:628–33.
[11] Raghunathan S. The wells turbine for wave energy conversion. Prog Aerosp Sci 1995;31:335–86.
[12] Evans DV. Wave power absorption by systems of oscillating pressure distributions. J Fluid Mech 1982;114:481–99.
[13] Sarmento AJNA, Falcão AFde O. Wave generation by an oscillating surface–pressure and its application in wave–energy extraction. J Fluid Mech 1985;150:467–85.
[14] Evans DV, Porter R. Hydrodynamic characteristics of an oscillating water column device. Appl Ocean Res 1995;17:155–64.
[15] Martins-Rivas H, Mei CC. Wave power extraction from an oscillating water column at the tip of a breakwater. J Fluid Mech 2009;626:395–414.
[16] Martins-Rivas H, Mei CC. Wave power extraction from an oscillating water column along a Straight Coast. Ocean Eng 2009;36:426–33.
[17] Lovas S, Mei C, Liu Y. Oscillating water column at a coastal corner for wave power extraction. Appl Ocean Res 2010;32:267–83.
[18] Mendoza E, Dias J, Didier E, Fortes CJEM, Neves MG, Reis MT, Conde JMP, Poseiro P, Teixeira PRF. An integrated tool for modelling oscillating water column (OWC) wave energy converters (WEC) in vertical breakwaters. J Hydro-Environ Res 2017. http://dx.doi.org/10.1016/j.jher.2017.10.007.
[19] Gato LMC, Falcão AFde O. Aerodynamics of the wells turbine: Control by swinging rotor blades. Int J Mech Sci 1989;31(6):425–34.
[20] Justino PAP, Falcão AFde O. Rotational speed control of an OWC wave power plant. J Offshore Mech Arct Eng 1999;121:65–70.
[21] Falcão AFde O, Justino PAP. OWC wave energy devices with air flow control. Ocean Eng 1999;26:1275–95.
[22] Carballo R, Sánchez M, Ramos V, Fraguela JA, Iglesias G. The intra-annual variability in the performance of wave energy converters: A comparative study in N Galicia (Spain). Energy 2015;82:138–46.
[23] Falcão AFde O, Henriques JCC, Gato LMC. Rotational speed control and electrical rated power of an oscillating-water-column wave energy converter. Energy 2016;120:253–61.
[24] López I, Pereiras B, Castro F, Iglesias G. Optimisation of turbine-induced damping for an OWC wave energy converter using a RANS-VOF numerical model. Appl Energy 2014;127:105–14.
[25] López I, Pereiras B, Castro F, Iglesias G. Performance of OWC wave energy converters: Influence of turbine damping and tidal variability. Int J Energy Res 2015;39(4):472–83.
[26] Rezanejad K, Bhattacharjee J, Guedes-Soares C. Stepped sea bottom effects on the efficiency of nearshore oscillating water column device. Ocean Eng 2013;70:25–38.
[27] Rezanejad K, Bhattacharjee J, Guedes Soares C. Analytical and numerical study of dual-chamber oscillating water columns on stepped bottom. Renew Energy 2015;75:272–82.
[28] Medina-López E, Bergillos RJ, Moñino A, Clavero M, Ortega-Sánchez M. Effects of seabed morphology on oscillating water column wave energy converters. Energy 2017;135:659–73.
[29] Medina-López E, Moñino A, Bergillos RJ, Clavero M, Ortega-Sánchez M. Oscillating water column performance under the influence of storm development. Energy 2019;166:765–74.
[30] Teixeira P, Davyt D, Didier E, Ramalhais R. Numerical simulation of an oscillating water column device using a code based on Navier–Stokes equations. Energy 2013;61:513–30.
[31] Luo Y, Nader JR, Cooper P, Zhu SP. Nonlinear 2D analysis of the efficiency of fixed oscillating water column wave energy converters. Renew Energy 2014;64:255–65.
[32] Moñino A, Medina-López E, Clavero M, Benslimane S. Numerical simulation of a simple OWC problem for turbine performance. Int J Mar Energy 2017;20:17–32.
[33] Halder P, Samad A. Optimal wells turbine speeds at different wave conditions. Int J Mar Energy 2016;16:133–49.
[34] Lopes BS, Gato LMC, Falcão AFde O, Henriques JCC. Test results of a novel twin-rotor radial inflow self-rectifying air turbine for OWC wave energy converters. Energy 2019;170:869–79.
[35] Cui Y, Liu Z, Zhang X, Xu C, Shi H, Kim K. Self–starting analysis of an OWC axial impulse turbine in constant flows: Experimental and numerical studies. Appl Ocean Res 2019;82:458–69.
[36] Liu Z, Cui Y, Xu C, Sun L, Li M, Jin J. Transient simulation of OWC impulse turbine based on fully passive flow-driving model. Renew Energy 2019;117:459–73.
[37] The Carbon Trust. Oscillating water column wave energy converter evaluation report. Mar Energy Chall 2005;196.
[38] Heras-Saizarbitoria I, Zamanillo I, Laskurain I. Social acceptance of ocean wave energy: a case study of an OWC shoreline plant. Renew Sustain Energy Rev 2013;27:515–24.
[39] Hitzeroth M, Megerle A. Renewable energy projects: Acceptance risks and their management. Renew Sustain Energy Rev 2013;27:576–84.
[40] Uihlein A, Magagna D. Wave and tidal current energy - A review of the current state of research beyond technology. Renew Sustain Energy Rev 2015;58:1070–81.
[41] de Andres A, Medina-Lopez E, Crooks D, Roberts O, Jeffrey H. On the reversed LCOE calculation: design constraints for wave energy commercialization. Int J Mar Energy 2017;18(2017):88–108.
[42] National Ocean Economic Program. Off–shore renewable energy. 2017, http://www.oceaneconomics.org/offshore_renewables/costs/.
[43] Jalón L, María L, Baquerizo A, Losada MA. Optimization at different time scales for the design and management of an oscillating water column system. Energy 2016;95:110–23.
[44] Stefanakos CN, Athanassoulis GS, Cavaleri L, Bertotti L, Lefevre JM. Wind and wave climatology of the mediterranean sea. Part II: Wave statistics. In: Proceedings of the fourteenth international offshore and polar engineering conference, Toulon, France, May 23-28. 2004.
[45] Rahman MM, Ibrahim-Thamir K, Kadirgama K, Mamat R, Bakar-Rosli A. Influence of operation conditions and ambient temperature on performance of gas turbine. Adv Mater Res 1995;189–193:3007–13.
[46] Kim TS, Song CH, Ro ST, Kauh SK. Influence of ambient condition on thermodynamic performance of the humid air turbine cycle. Energy 1991;4(4):313–24.
[47] Yang W, Su M. Influence of moist combustion gas on performance of a sub-critical turbine. Energy Convers Manage 2004;46:821–32.
[48] Singh S, Kumar R. Ambient air temeprature effect on power plant performance. Int J Eng Sci Technol 2012;4(8):3916–28.
[49] Zhang Y, Zou QP, Greaves DM. Air water two–phase flow modelling of hydrodynamic performance of an oscillating water column device. Renew Energy 2012;49:159–70.
[50] Sheng W, Alcorn R, Lewis S. On thermodynamics of primary energy conversion of OWC wave energy converters. Renew Sustain Energy 2013;5:023105.
[51] Gayé Biel J. Formalismo y método de la termodinámica. Teoría general, aplicaciones y ejercicios resueltos. Apuntes de clase. Universidad de Granada; 1986, p. 258.
[52] Prausnitz J, Lichtenthaler R, Gomes de Azevedo E. Molecular thermodynamics of fluid–phase equilibria. 1999, p. 864.
[53] Wisniak J. Heike kamerlingh – the virial equation of state. Indian J Chem Technol 2003;10:564–72.
[54] Tsonopoulos C, Heidman JL. From the virial to the cubic equation of state. Fluid Phase Equilib 1990;57:261–76.
[55] Medina-López E, Moñino A, Clavero M, Del Pino C, Losada MA. Note on a real gas model for OWC performance. Renew Energy 2016;85:588–97.
[56] Medina-López E, Moñino A, Borthwick AGL, Clavero M. Thermodynamics of an OWC containing real gas. Energy 2017;135:709–17.
[57] Medina-López E, Borthwick A, Moñino A. Analytical and numerical simulations of an oscillating water column with humidity in the air chamber. J Clean Prod 2019;238:117898.
[58] Huertas-Fernández F, Clavero M, Reyes-Merlo MA, Moñino A. Combined oscillating water column & hydrogen electrolysis for wave energy extraction and management. A case study: The port of motril (Spain). J Clean Prod 2021;324:129143.
[59] Rosen MA. Energy and exergy analyses of electrolytic hydrogen production. Int J Hydrog 1995;20(7). 547–533.

[60] Sciubba E. A brief commented history of exergy. From the beginnings to 2004. Int J Thermodyn 2007;10(1):1–26.
[61] de Oliveira Jr S. Exergy. Production, cost and renewability. Springer; 2013, p. 336.
[62] Arredondo Hector Ivan Velasquez, Pellegrini Felipe Luiz, Oliveira Junior, et al. Ethanol and sugar production process from sugar cane: renewability evaluation. In: Conference: ENCIT, Vol. 12. Rio de Janeiro, RJ (Brazil): Associacao Brasileira de Engenharia e Ciencias Mecanicas (ABCM); 2008.
[63] Moñino A, Quirós C, Mengíbar F, Medina-López E, Clavero M. Thermodynamics of the OWC chamber: Experimental turbine performance under stationary flow. Renew Energy 2020;155:317–29.
[64] Molina-Salas A, Jiménez-Portaz M, Clavero M, Moñino A. The effect of turbine characteristics on the thermodynamics and compression process of a simple OWC device. Renew Energy 2022. http://dx.doi.org/10.1016/j.renene.2022.03.106.